

Simulation of the Metamorphic and Deformational History of the Metamorphic Sole of the Oman Ophiolite

BRADLEY R. HACKER¹

Department of Earth and Space Sciences, University of California, Los Angeles

Emplacement of ophiolites onto less dense continental crust is an enigma. The rates of emplacement, the mechanisms of emplacement, and the stress and temperature histories of the rocks are all incompletely understood. The Oman ophiolite is well exposed and has been studied extensively by field geologists. An integrated thermal and kinematic model of the temperature, stress, rock type, and displacement fields during the early stages of the emplacement of the Oman ophiolite is developed here to explain field relations and provide insight into the development of the metamorphic rocks at the base of the ophiolite. The thermal evolution was calculated by a finite difference algorithm for heat conduction, considering heats of metamorphic reactions, deformational heating, and heat advection by rock. The stress and displacement fields were calculated by an analytical model using a velocity boundary condition, power law constitutive relations, and a brittle frictional sliding relationship. In simulations involving young, hot subducted lithosphere, a wider portion of the subduction zone deforms by power law creep, and deformation occurs at lower stresses and slower strain rates, minimizing the deformational heating compared to colder, older subducted lithosphere. Dehydration occurs at an accelerated rate in younger, hotter lithosphere, removing heat from the subducted plate at an earlier stage and causing the zone of brittle deformation to propagate downward more rapidly. Power law creep of subducted basaltic rocks is limited to temperatures greater than 500°C and occurs at differential stresses of the order of 100 MPa. The simulations predict that metamorphic field gradients and the spatial distribution of rock types in the metamorphic sole of Tethyan ophiolites might be used to infer the emplacement direction of the ophiolite.

INTRODUCTION

The mechanisms by which nappes of oceanic lithosphere tens of thousands of square kilometers in area and as much as 20 km thick are emplaced onto less dense continental crust remain somewhat obscure. Tethyan-type ophiolites are emplaced onto continental margins by subduction of the edge of a continent beneath an immature arc [e.g., *Moore*, 1982], but the evolution of the deformation and metamorphism in such a convergence zone is poorly understood. Many ophiolite nappes are bounded below by soles, or basal fault zones, which consist of high-temperature metamorphic rocks. These soles have been inferred by numerous geologists to have formed when hot young oceanic lithosphere was thrust over colder older lithosphere [e.g., *Williams and Smyth*, 1973; *Jamieson*, 1986]. They contain inverted metamorphic field gradients as extreme as 1000 K km⁻¹, grading from mylonitic peridotite downward through granulite-, amphibolite-, and greenschist-facies rocks into unmetamorphosed material. Many soles also preserve an "inverted ophiolite," with metamorphosed gabbroic(?) and diabasic rocks overlying pillow basalts and chert. These soles provide the key to understanding ophiolite emplacement because their metamorphic parageneses and textures record their metamorphic and deformational history. The purpose of this paper is to present a model of the early stages of the thermal and kinematic history of the sole of the Oman ophiolite, to test aspects of the ophiolite emplacement hypothesis of *Lippard et al.* [1986], and to illustrate how a physical model using laboratory measurements can replicate

field observations and provide new insights into interpreting field data. No previous thermomechanical models of the metamorphic soles of ophiolites have been presented, although *Jamieson* [1986] suggested that such work would be fruitful.

Moore [1982] divided ophiolites into two types: Tethyan and Cordilleran. Most Tethyan-type ophiolites contain metamorphic soles similar to the Oman ophiolite [*Jamieson*, 1986]; hence the results of this study are broadly applicable to other Tethyan-type ophiolites. Cordilleran-type ophiolites are smaller and are often fragments within accretionary wedges; the results of this study are not applicable to Cordilleran-type ophiolites because of these differences.

GEOLOGY OF THE OMAN OPHIOLITE

Most Tethyan ophiolites were thrust onto the African-Arabian platform in Cretaceous time and then further deformed and metamorphosed during the continent-continent collision that ended the Alpine orogeny [*Lippard et al.*, 1986]. The Oman ophiolite, however, was spared the effects of the continent-continent collision and constitutes a natural laboratory for investigating ophiolites. Diverse field studies of the Oman ophiolite have been published, including four journal issues or volumes dedicated to the Oman ophiolite [*Glennie et al.*, 1974; *Coleman and Hopson*, 1981; *Lippard et al.*, 1986; *Boudier and Nicolas*, 1988].

The Oman Mountains comprise a west directed system of oceanic nappes (Figure 1) that were thrust over a Precambrian to Cretaceous continental autochthon in Cretaceous time and then overlapped by Upper Cretaceous sedimentary rocks. The autochthon includes continental shelf rocks of the Arabian platform resting on cratonal rocks as old as 858±16 Ma (Rb-Sr whole rock [*Glennie et al.*, 1974]). The nappes are, from structurally lowest (westernmost) to structurally highest (easternmost), the Sumeini Group, the Hawasina Assemblage, the Haybi Complex, the ophiolite, and the Batinah Complex. The Sumeini, Hawasina, and Haybi are continental slope,

¹Now at Department of Geology, Stanford University, Stanford California.

Copyright 1990 by the American Geophysical Union.

Paper number 89JB03450.
0148-0227/90/89JB-03450\$05.00

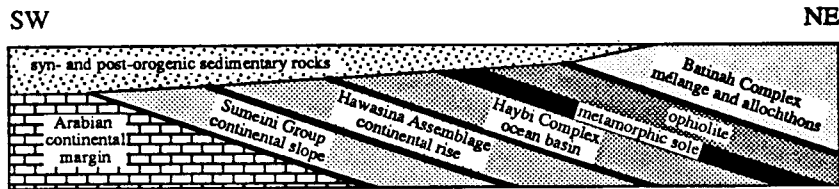


Fig. 1. Schematic illustration of the nappes in the Oman Mountains.

continental rise, and pelagic sedimentary rocks, respectively, deposited in a Middle Triassic to Late Cretaceous passive margin and ocean basin northeast of the Arabian craton [Glennie *et al.*, 1974; Woodcock and Robertson, 1982a; Lippard *et al.*, 1986; Béchennec *et al.*, 1988]. The ophiolite, now disrupted into a number of relatively intact blocks, exposes a classic ophiolite pseudostratigraphy as recognized by the *Penrose Conference Participants* [1972]. The Batinah Complex includes mélange derived from beneath the ophiolite during late stage extensional faulting and allochthonous thrust sheets of sedimentary rocks that slid onto the ophiolite late in the emplacement history [Woodcock and Robertson, 1982b; Robertson and Woodcock, 1983a].

The presently exposed ophiolite extends more than 600 km and is up to 150 km wide and 5-10 km thick. It is inferred to have been 16-20 km thick (Figure 2) prior to its dismemberment on the craton by extensional faulting. The nappe consists of a metamorphic sole (≤ 500 m), peridotite tectonite (8-12 km), plutonic peridotite and gabbro (0.5-6.5 km), sheeted dikes (1-1.5 km), lavas (0.5-2.0 km), and pelagic sedimentary rocks (≤ 100 m) [Boudier and Coleman, 1981; Christensen and Smewing, 1981; Manghnani and Coleman, 1981; Pallister and Hopson, 1981; Lippard *et al.*, 1986]. The metamorphic sole is the thrust zone at the base of the

ophiolite, comprising partially melted lower granulite/upper amphibolite to lower greenschist facies rocks. The least disrupted exposures of the metamorphic rocks contain ≤ 300 m of amphibolite-facies rocks and ≤ 300 m of greenschist-facies rocks. The majority of the amphibolites are intermediate in composition between normal mid-ocean ridge basalts and within-plate tholeiites, similar to volcanic rocks in the underlying Haybi Complex [Lippard *et al.*, 1986]. Peak metamorphic temperatures are estimated as 765° - 875° C [Ghent and Stout, 1981], and the amphibolite-facies rocks are overprinted by greenschist-facies assemblages. The amphibolite-facies rocks are gneissic to schistose, and amphibole and plagioclase crystals contain crystal-plastic deformation features. Greenschist-facies rocks underlying the amphibolites include metamorphosed sandstone, shale, limestone, chert, and volcanic rocks, perhaps derived from the Hawasina Assemblage or the Haybi Complex. Initial metamorphism of the greenschist-facies rocks occurred during deformation, producing a penetrative schistosity, and later minerals grew during static conditions [Lippard *et al.*, 1986]. The amphibolite- and greenschist-facies rocks (Figure 3) yield K-Ar and $^{40}\text{Ar}/^{39}\text{Ar}$ cooling ages from ~ 100 to 70 Ma [Alleman and Peters, 1972; Searle *et al.*, 1980; Lanphere, 1981; Montigny *et al.*, 1988]. Many of the dates from amphibolite-facies rocks span a 6-m.y. interval from 101 to 95 Ma.

The peridotite tectonite, plutonic peridotite and gabbro, sheeted dikes, and lowermost lavas represent oceanic lithosphere of "normal" chemistry and thickness [Alabaster *et al.*, 1982; Lippard *et al.*, 1986; Ernewein *et al.*, 1988]. Eleven ^{206}Pb - ^{238}U ages on plagiogranites in the intrusive sequence are

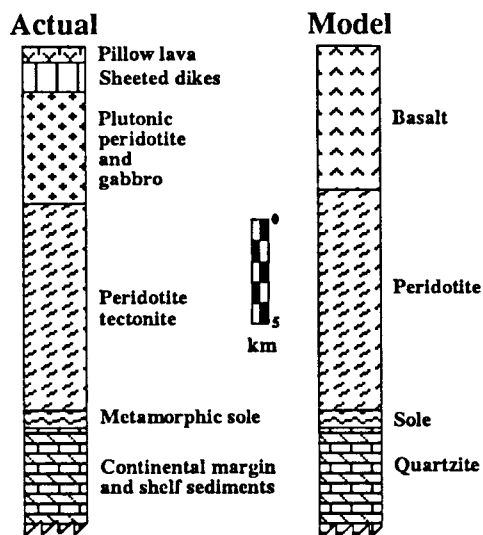


Fig. 2. A pseudostratigraphic section of the Oman ophiolite and the simplified section used in the model. Sections measured in the field have 0.5-2.0 km of pillow lava, 1.0-1.5 km dikes, 0.5-6.5 km plutonic peridotite and gabbro, 8-12 km peridotite tectonite, and 0-0.5 km of metamorphic rocks [Boudier and Coleman, 1981; Christensen and Smewing, 1981; Manghnani and Coleman, 1981; Pallister and Hopson, 1981; Lippard *et al.*, 1986]. The pseudostratigraphic section is a composite reconstruction based on numerous incomplete sections and is inferred to represent the pseudostratigraphy of the ophiolite before disruption.

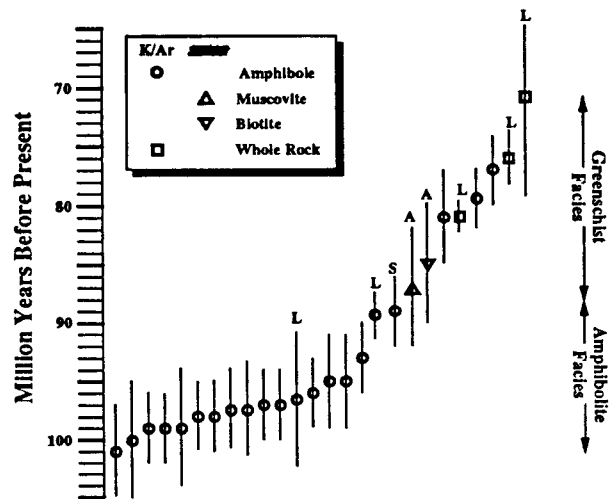


Fig. 3. Radiometric data from the metamorphic sole of the Oman ophiolite. All data are from Montigny *et al.* [1988], except for data labeled "L" [Lanphere, 1981], "A" [Alleman and Peters, 1972], and "S" [Searle *et al.*, 1980]. Mean values and one-sigma standard deviations are shown as symbols and lines.

in the range 95.4-93.5±0.5 Ma, although there are two that are slightly older: 96.9 and 97.3 Ma [Tilton *et al.*, 1981]. Unfortunately, these plagiogranites may have been derived from partial melting of the amphibolite-facies sole rocks (compare with Figure 3) and may not date the igneous crystallization of the ophiolite. Two foliations have been mapped in the peridotite: (1) a pervasive coarse porphyroclastic foliation, and (2) a fine-grained porphyroclastic to mylonitic foliation in the lower 150-2000 m of the peridotite, which overprints the pervasive foliation and increases in intensity downward toward the metamorphic sole [Searle *et al.*, 1980; Nicolas *et al.*, 1980; Boudier and Coleman, 1981; Boudier *et al.*, 1988; Ceuleneer *et al.*, 1988]. The pervasive foliation is inferred to have formed during high-temperature, low-stress asthenospheric flow, and the mylonitic foliation is inferred to have formed at lower temperatures and higher stresses during the emplacement of the ophiolite [Boudier and Coleman, 1981]. Olivine microstructures and two-pyroxene thermometry have been used to infer temperatures of mylonitization of 750°-1000°C [Boudier and Coleman, 1981; Lippard *et al.*, 1986; Ceuleneer *et al.*, 1988].

There is controversy concerning the type of tectonic environment in which the middle and upper lavas of the Oman ophiolite were erupted. Pearce *et al.* [1981] and Lippard *et al.* [1986] interpret the Oman ophiolite as part of an arc, whereas Ernewein *et al.* [1988], Montigny *et al.* [1988], Nicolas *et al.* [1988], Boudier *et al.* [1988], and Thomas *et al.* [1988] believe that the ophiolite is normal oceanic lithosphere. This paper addresses the former of these two possibilities; consideration of the latter alternative awaits future modeling.

TECTONIC EVOLUTION OF THE OMAN OPHIOLITE

The field observations described above suggest the following tectonic evolution of the Oman ophiolite. In Late Permian time a large intracratonal basin formed on the northeast portion of the Arabian platform [Lippard *et al.*, 1986; Boudier and Nicolas, 1988]. Rifting of the basin and subsequent creation of oceanic lithosphere in Middle to Late Triassic time resulted in terrigenous turbidite deposition succeeded by Middle Jurassic calcareous turbidite and chert deposition. In Late Jurassic to Early Cretaceous time, slow pelagic sedimentation was dominant. Radical change occurred in Albian to Cenomanian time, when intraoceanic subduction initiated. Metamorphism in the ophiolite sole spanned Albian to Campanian time (101-70 Ma). During this interval, the allochthonous nappes were assembled and faulted onto the Arabian continental margin. By Maastrichtian time (70-65 Ma), all the nappes had been partially eroded and transgressed by shallow water carbonate rocks. These parts of the ophiolite development are agreed upon by most authors [Lippard *et al.*, 1986; Boudier and Nicolas, 1988]. However, as mentioned previously, there is disagreement regarding the petrogenesis and tectonic implications of the middle and upper lavas. Lippard *et al.* [1986, p. 155] suggest that the ophiolite evolved on the west flank of a back-arc spreading center above a subduction zone dipping away from the continent (Figure 4). They propose that the intraoceanic subduction initiated at the contact between the young crust and the older (5-100 m.y. older) oceanic lithosphere in which it formed; the contact between the younger and older lithosphere would be a likely place for the initiation of subduction because of the density contrast. In contrast, Montigny *et al.* [1988, p. 359], Ernewein *et al.* [1988, p. 270], Nicolas *et al.* [1988, p. 51],

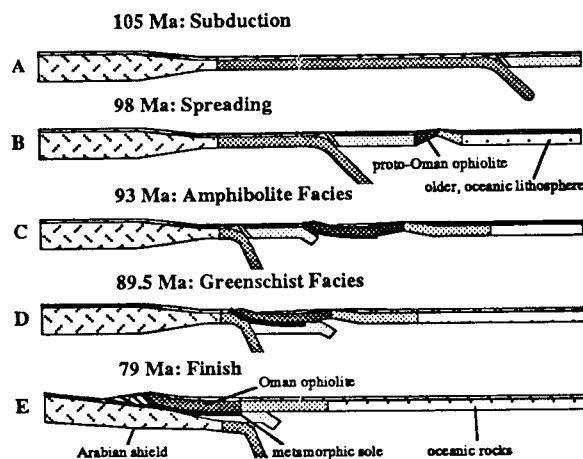


Fig. 4. Hypothetical palinspastic reconstruction of the genesis and emplacement of the Oman ophiolite [after Lippard *et al.*, 1986]. (a) 105 Ma: Subduction begins in the ocean basin at 50 mm yr⁻¹; the oldest oceanic crust was 110 m.y. old at this time, and the continental crust was 750 m.y. old. (b) 98 Ma: Spreading begins above the subducting plate, forming the oldest igneous rocks in the ophiolite. (c) 93 Ma: The ophiolite is thrust over older oceanic rocks, which are accreted at amphibolite-facies grade to the base of the ophiolite, shown by a heavy line. (d) 89 Ma: The ophiolite is thrust over continental rocks, which are accreted at greenschist-facies grade to the base of the ophiolite. (e) 79 Ma: Convergence is complete. The simulations reported in this paper refer only to stages in Figures 4c and 4d. Note that the most recently published dates on the metamorphic sole [Montigny *et al.*, 1988] suggest that the period of amphibolite-facies metamorphism spanned ~11 m.y., and consequently, the dates specified in Lippard *et al.*'s model are probably incorrect even though the basic geometry may be correct.

Boudier *et al.* [1988, p. 289], and Thomas *et al.* [1988, p. 318] suggest that the ophiolite originated on the east flank of a mid-ocean spreading center and that intraoceanic subduction was initiated at the ridge axis.

THE MODEL

A thermomechanical model was developed to test part of the tectonic history proposed by Lippard *et al.* [1986]. Specifically, the model predicts the stress-, temperature-, rock-type and displacement-field histories during the early stages of the emplacement of the Oman ophiolite. Lippard *et al.* [1986, pp. 153-156] propose that subduction dipping away from the continental margin began at ~105 Ma (Figure 4a) and spreading above the subduction zone formed the Oman ophiolite (Figure 4b). Later, when continental lithosphere reached the subduction zone, subduction stepped away from the continent to the contact between the young ophiolite and the older oceanic lithosphere that it had intruded (Figure 4c). Basaltic rocks from the underthrust plate were metamorphosed at amphibolite-facies conditions and accreted to the base of the ophiolite (Figure 4c), and then continental material was accreted to the sole at greenschist-facies conditions (Figure 4d). Note that more recent radiometric dating by Montigny *et al.* [1988] suggests a lengthier period of amphibolite-facies metamorphism. The convergence velocity was assumed to be initially ~70 mm yr⁻¹, declining to ~30 mm yr⁻¹ within 2 m.y. The total amount of oceanic lithosphere subducted beneath the ophiolite is estimated as 100 km by assuming that the subduction zone magmas were produced at ~100 km depth and that the subduction zone dipped 45°. The total amount of continental lithosphere subducted is estimated as 180 km, from

the width of the ophiolite outcrop on the Arabian platform. The subducted oceanic lithosphere was between 5 and 100 m.y. old at the time of subduction, and the subducted continental lithosphere was 768 m.y. old [Lippard *et al.*, 1986]. The convergence velocity and total subducted lithosphere are estimates of Lippard *et al.* [1986]; neither estimate is likely to be correct, but the present simulations are unable to assess their validity.

Thermal Model

Calculations were made for a cross section 34 km thick and 100 km long of oceanic rocks (Figure 5). The upper plate ophiolite occupied roughly the upper right portion of this area, and the lower plate subducted material began to the left and was subducted beneath the upper plate. The cross section was divided into nodes spaced 1 km vertically and 2 km horizontally. Between depths of 16 and 19 km, where most of the deformation occurred, the vertical node spacing was 100 m.

The thermal evolution was evaluated by solving the conservation of energy equation with a two-dimensional alternating-direction implicit finite difference algorithm. Heat conduction, heats of metamorphic reactions, deformational heating, and advection of heat by rock displacement were taken into account, whereas kinetic energy was neglected. The mass-dependent local heat production includes only heats of metamorphic reactions; radioactive heat production ($\sim 16^\circ \text{ m.y.}^{-1}$ for continental crust) and adiabatic compression ($\leq 5^\circ$ for a change in depth of ~ 20 km) are small [Toksöz *et al.*, 1971] and were ignored in this simulation. Heat was allowed to advect, but not conduct through the ends of the model.

The temperature field at the initiation of a simulation was calculated after Parsons and Sclater [1971] and depends only on the age of the lithosphere and the peridotite solidus (Figure 5). At the time of intraoceanic subduction the ophiolite was 5 m.y. old. The lithosphere subducted beneath the ophiolite was between 5 and 100 m.y. old [Lippard *et al.*, 1986]; in order to make the differences between subduction of 5-m.y.-old and 100-m.y.-old lithosphere clear, the geometry of subduction was assumed to be the same for both cases. The assumed geometry might be appropriate for young lithosphere but is unlikely to be appropriate for old lithosphere.

Heat was not allowed to conduct across the boundary between the two plates before intraoceanic subduction began. This was not a simplification in simulations where the plates are the same age, because the thermal structures of both plates are identical. For simulations with a 100-m.y.-old plate subducted beneath a 5-m.y.-old plate, however, there was a large

horizontal step in the thermal gradients before subduction began (Figure 5). Although the total amount of heat was the same, this thermal step may produce some transient results that would not be present if some presubduction thermal conduction were allowed.

Rock Types

For the purpose of modeling, the pseudostratigraphy of the ophiolite (Figures 2 and 5) was simplified to a 7-km basaltic layer and a 10-km peridotite layer. Because of small thickness (< 100 m), the pelagic sediments overlying the Oman ophiolite [Robertson and Woodcock, 1983b; Lippard *et al.*, 1986] were ignored. The nodes in the basaltic layer were assumed to contain mineral assemblages appropriate to their pressure and temperature: either prehnite-pumpellyite, greenschist-, or amphibolite-facies minerals (see below). The initial thermal gradient for 5-m.y.-old lithosphere [Parsons and Sclater, 1971] was such that the upper 3 km of the basaltic layer were prehnite-pumpellyite facies, and the lower 4 km were greenschist facies. There were no amphibolite-facies nodes at the beginning of a simulation; they formed only through heating.

Thermal Parameters

Thermal properties of the prehnite-pumpellyite, greenschist-, and amphibolite-facies basaltic rocks were calculated from reported modal mineralogies of layer 2B of oceanic crust (zeolite-facies tholeiite), layer 3A of oceanic crust (greenschist-facies gabbro), amphibolite-facies gabbro, and peridotite (Table 1). The densities of these rocks, 2750-3250 kg m^{-3} (Table 1), were represented in the model by an average density of 3000 kg m^{-3} . Calculated heat capacities for these four rock types range from 1057 to 1293 $\text{J kg}^{-1} \text{K}^{-1}$; a heat capacity of 1200 $\text{J kg}^{-1} \text{K}^{-1}$ was used in the model.

A single value of thermal conductivity was used for the entire model; this was a necessary simplification because thermal diffusivities and conductivities are not well determined for all the rocks considered in this study. Durham *et al.* [1987] found thermal diffusivities for one basalt and two gabbros in the range $0.53\text{-}1.03 \times 10^{-6} \text{ m}^2 \text{ s}^{-1}$ for temperatures of $100^\circ\text{-}800^\circ\text{C}$, and in the range $0.61\text{-}0.79 \times 10^{-6} \text{ m}^2 \text{ s}^{-1}$ for temperatures of $350^\circ\text{-}550^\circ\text{C}$. For rocks with heat capacities of 1057-1293 $\text{J K}^{-1} \text{ kg}^{-1}$, a density of 3000 kg m^{-3} , and thermal diffusivities of $0.5\text{-}1.0 \times 10^{-6} \text{ m}^2 \text{ s}^{-1}$, the thermal conductivity is 1.6-3.9 $\text{J K}^{-1} \text{ m}^{-1} \text{ s}^{-1}$. Measured thermal conductivities of basalt, diabase, gabbro, dunite, and amphibolite all fall in the range 2.1-2.9 $\text{J K}^{-1} \text{ m}^{-1} \text{ s}^{-1}$ [Clark, 1966]. The thermal conductivity of one

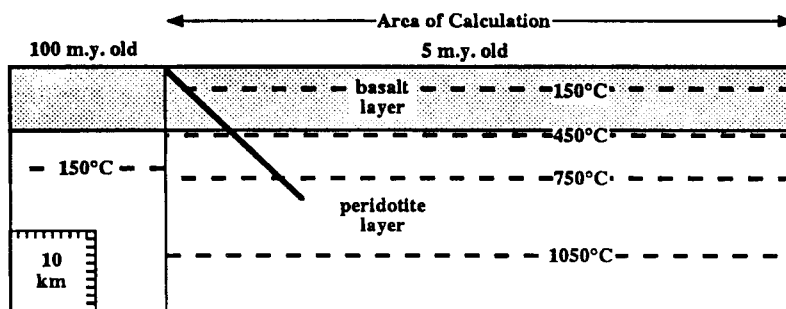


Fig. 5. Initial conditions of a simulation where 100-m.y.-old lithosphere is subducted beneath 5-m.y.-old lithosphere. The plate on the left represents the older lithosphere to be subducted beneath the younger plate on the right. The heavy diagonal line marks the predefined 45° trace of the upper, brittle portion of the subduction zone.

TABLE 1. Thermal Properties of Rock Types in the Model

Rock Type	Composition	Density		Heat Capacity		H ₂ O, wt %
		kg m ⁻³	kg mol ⁻¹	J mol ⁻¹ K ⁻¹	J kg ⁻¹ K ⁻¹	
Layer 2B	ab ₂₄ ep ₃₃ ch ₂₀ ac ₂₀ qz ₀₃	2,750	0.418	498	1,057	3.5
Layer 3A	an ₆₃ ch ₁₆ ac ₁₆ en ₀₅	2,875	0.368	477	1,293	2.5
Gabbro	pg ₁₆ at ₁₆ tr ₁₇ ab ₂₅ an ₂₅	2,950	0.534	628	1,176	1.0
Harzburgite	fo ₇₄ en ₂₄ sp ₀₂	3,250	0.134	172	1,283	0.0

Compositions of layers 2B and 3A are from *Anderson et al.* [1976]; the peridotite (harzburgite) composition is taken from *Boudier and Coleman* [1981]. Minerals abbreviations are ab, albite; ac, actinolite; an, anorthite; at, anthophyllite; ch, chlorite; ep, epidote; fo, forsterite; qz, quartz; en, enstatite; pg, pargasite; sp, spinel; and tr, tremolite. Rock densities are estimated from mineral densities of *Clark* [1966] and *Carmichael* [1984], and porosities given by *Newmark et al.* [1985]. The heat capacities are calculated using the virial constants of *Helgeson et al.* [1978] and considering temperatures of 100°-400°C and pressures of 0-200 MPa for layer 2B, 300°-700°C and 0-400 MPa for layer 3A, 400°-700°C and 0-400 MPa for amphibolite, and 700°-1200°C and 0-400 MPa for harzburgite.

synthetic basalt measured by *Toksöz et al.* [1972] was 1.25-2.09 J m⁻¹ s⁻¹ K⁻¹. Thus the variations in measured and calculated values indicate that relevant thermal conductivities are in the range of 1.25-3.9 J K⁻¹ m⁻¹ s⁻¹; a conductivity of 3 J K⁻¹ m⁻¹ s⁻¹ was used in the present study.

The rock types change through metamorphic reactions, which release or consume heat. In the model, the zeolite ↔ greenschist and greenschist ↔ amphibolite transitions occur instantaneously at 250°C and 450°C, respectively. *Anderson et al.* [1976] calculated that dehydration of oceanic layer 2B (zeolite facies with 3.5 wt % H₂O) consumes 4.42 × 10⁸ J m⁻³, and dehydration of layer 3A (greenschist facies with 2.5 wt % H₂O) requires 1.98 × 10⁸ J m⁻³. A value of 2.44 × 10⁸ J m⁻³ was used for the dehydration of zeolite-facies zeolite-facies rocks (2.44=4.42-1.98), and 1.2 × 10⁸ J m⁻³ for dehydration of greenschist-facies rocks to form amphibolite (1 wt % H₂O).

Metamorphic parageneses and volatile contents of oceanic crust are incompletely known [*Peacock*, 1987b]. The heats of metamorphic reactions are strongly dependent on the amount of water evolved, and it is possible that other heats of reaction for oceanic crust would be more appropriate. *Peacock* [1987a, b] modeled the thermal effects of metamorphic fluids in subduction zones, choosing dehydration reactions releasing 2% H₂O, compared to the 1.5% used in the present study. The present study does not include the effects of fluid flow or retrograde hydration reactions in the over-riding plate; see *Peacock* [1987b] for such an analysis. The zeolite ↔ greenschist and greenschist ↔ amphibolite transitions occur in the model instantaneously at 250°C and 450°C, whereas most minerals in basaltic rocks are solid solutions and participate in continuous reactions that span a range of temperatures. Future models could investigate the effects of discontinuous reactions, although the dense spacing of isotherms may render any improvement minimal.

The metamorphic history of the Oman Mountains is complicated by high-pressure metamorphism in addition to the high-temperature-low-pressure metamorphism along the metamorphic sole. Eclogite and blueschist crop out in a 10 by 40 km area in the Oman Mountains [*Goffé et al.*, 1988]. These rocks are interpreted to have formed during imbrication of the continental margin prior to their subduction beneath the ophiolite [*Montigny et al.*, 1988]. This imbrication is dated as coeval with or predating the amphibolite-facies metamorphism in the metamorphic sole [*Montigny et al.*, 1988]; K-Ar and ⁴⁰Ar/³⁹Ar dates on phengite range from 131 to 80 Ma with two clusters at ~115-100 Ma and 93-78 Ma [*Montigny et al.*,

1988]. This metamorphism is spatially distinct from the metamorphism in the sole and was not considered in the present study.

Mechanical Parameters

The stress and displacement fields were calculated with an analytical model using velocity boundary conditions, temperature-dependent power law constitutive relations, and a pressure-dependent brittle frictional sliding relationship. The horizontal velocity boundary condition specifies the rate at which material is subducted beneath the ophiolite. The stress estimate is the result of the velocity boundary condition and the rheology of the rocks. The displacement field defines the advection and determines where the deformation occurs.

The strength of rock was computed as a function of pressure, temperature, strain rate, and rock type. Three modes of deformation were considered: (1) brittle frictional sliding, (2) power law creep (Table 2), and (3) transitional behavior (Figure 6). Whichever mode of deformation required the lowest stress at a given node (i.e., at a given pressure, temperature, and rock type) was considered to be the only active mode of deformation at that node. At low temperatures and pressures, brittle failure occurs because power law creep strengths are large at low temperatures, whereas the brittle strength is small at low pressures and assumed to be independent of temperature. At high temperatures and pressures, power law creep occurs because the brittle strength is large at high pressures, whereas power law creep strengths are low at high temperatures and assumed to be independent of pressure.

The brittle strength calculation was based on *Brace and Kohlstedt's* [1980] suggestion (using *Byerlee's* [1968] "law") that the shear traction necessary to overcome static friction in prefaulted rock depends on the normal traction, and is independent of temperature, rock type and strain rate. This relationship was restated by *Kirby* [1983] for a rock containing fractures of all orientations, as

$$\begin{aligned} \sigma &= 4 \sigma_{zz} & \sigma_{zz} < 110 \text{ MPa} \\ \sigma &= 210 \text{ MPa} + 2.1 \sigma_{zz} & \sigma_{zz} \geq 110 \text{ MPa} \\ \sigma_{zz} &= \rho (1-\lambda) g z \end{aligned}$$

where ρ is the rock density, g is the gravitational acceleration, z is the depth, and λ is the ratio of fluid pressure to lithostatic pressure. Fluid pressure was assumed to be hydrostatic; the implications of this are discussed below. The inclination of the subduction zone in the shallow depths of the model where brittle deformation occurs was set at 45°. Subducted material beneath the 45° line was translated downward and to the right at 45° relative to the ophiolite in the upper plate.

TABLE 2. Power Law Constitutive Relationships

Parameter	Definition
$\dot{\epsilon}$	$A \sigma^n \exp(-H/RT)$
$\dot{\epsilon}$	$C \sigma^n \exp(-gT_m/T)$
$\dot{\epsilon}$	strain rate, s^{-1}
A, C	preexponential constant, $MPa n^{-1} s^{-1}$
σ	stress, MPa
H	activation enthalpy, $kJ mol^{-1}$
R	gas constant, $8.314 J K^{-1} mol^{-1}$
T	temperature, K
T_m	homologous temperature = $1580 K + 0.1 K MPa^{-1}$

Rock Type	A, C	n	H, g	Source
Quartzite	5.05×10^{-6}	2.61	145	Koch [1988] 9
Basalt	1.0×10^{-4}	3.5	250	combination of Shelton and Tullis [1981] and Hacker and Christie [1990]
Harzburgite	7.72	3.2	11.88	Borch and Green [1989]

Quartzite [Koch et al., 1989] and harzburgite [Borch and Green, 1989] flow laws were used to model power law creep of continental rocks and peridotite, respectively (Table 2). Power law creep of basaltic rocks was modeled using an approximate constitutive equation derived from experiments on diabase [Shelton and Tullis, 1981], and amphibolite [Hacker and Christie, 1990]. These power law constitutive relationships are functions of temperature and strain rate, and assumed to be independent of pressure.

In geological materials there is unlikely to be a direct transition from ductile dislocation (power law) creep to brittle frictional sliding, but instead the transition may involve some kind of behavior such as ductile cataclastic flow [Hadizadeh and Rutter, 1983; Tullis and Yund, 1987] and/or brittle dislocation creep [Carter and Tsenn, 1987]. Unfortunately, the stresses supported during such transitional behavior are unquantified experimentally. Modeling by Bird [1978] has suggested that deformation in upper crustal levels of subduction zones occurs at shear stresses no greater than 80 MPa. Other studies, including piezometry [e.g., Ord and Christie, 1984; Carter and Tsenn, 1987; Hacker et al., 1990], extrapolation of flow laws to active faults [Sibson, 1984], and calculation of stresses to support long-term loads [Kirby, 1983], suggest similar limits. In the present study, transitional behavior was defined to occur in all conditions where the brittle and power law creep strengths exceed 100 MPa shear stress. For the rock types, pressures, and temperatures in the simulations reported here, brittle behavior occurs at shallow depths (generally <15 km), power law creep occurs at great depths (≥ 15 km), and transitional behavior occurs at intermediate depths (15-17 km).

"Flow laws," or stress-temperature-strain rate constitutive relations, for rocks are derived from laboratory experiments. They must, in general use, be extrapolated to geologic strain rates. If a steady state geologic deformation occurs by the same mechanisms that operated during the experiments, then the constitutive relations can be used to predict one of the variables, temperature, stress, or strain rate, if the other two variables are known [Poirier, 1985]. Good experimental data are available for harzburgite [e.g., Borch and Green, 1989] and quartzite [e.g., Shelton and Tullis, 1981; Hansen, 1982; Hansen and Carter, 1982; Jaoul et al., 1984; Kronenberg and Tullis, 1984; Koch et al., 1989], but unfortunately, fewer experimental rheological data exist for basaltic rocks. Two features suggest that this limitation still allows reasonable plate scale modeling [Hacker and Christie, 1990]. First, the constitutive relations for diabase [Shelton and Tullis, 1981] and amphibolite [Hacker and Christie, 1990] yield similar predictions to other available "flow laws" for basaltic rocks [Caristan, 1982; Hansen and Carter, 1982]. Second, the stresses predicted by the constitutive relations for basaltic rocks are one order of magnitude less than stresses predicted

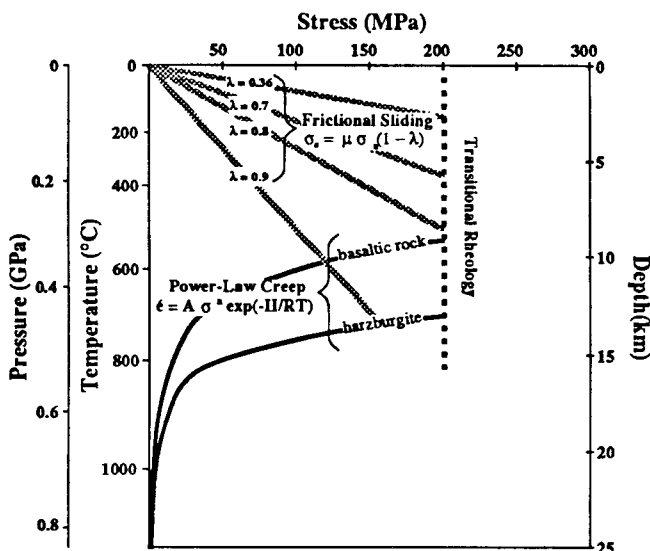


Fig. 6. Strength was determined as a function of pressure, temperature, and rock type. At shallow depths, low pressures, and low temperatures, frictional sliding occurs; the strength was determined by a relationship of the form: $\sigma_s = \mu \sigma_n (1-\lambda)$ (pressures are shown on the vertical axis, and the strain rate is $10^{-12} s^{-1}$). At great depths, high pressures, and high temperatures, power law creep occurs; the strength was determined by a relationship of the form: $\dot{\epsilon} = A \sigma^n \exp(-H/RT)$ or $\sigma = (\dot{\epsilon} / (A \exp(-H/RT)))^{1/n}$ (temperatures are shown on the vertical axis). A transitional regime occurs at intermediate depths where the frictional sliding and power law creep strengths exceed 200 MPa differential stress. λ , pore pressure fraction of total pressure; σ_s , shear traction; μ , friction; σ_n , normal traction; $\dot{\epsilon}$, strain rate; A , preexponential constant; σ , differential stress; n , stress exponent; H , activation enthalpy; R , gas constant; T , absolute temperature.

from harzburgite flow laws [e.g., *Borch and Green*, 1989] and 1-2 orders of magnitude larger than stresses predicted from six quartzite flow laws [*Shelton and Tullis*, 1981; *Hansen*, 1982; *Hansen and Carter*, 1982; *Jaoul et al.*, 1984; *Kronenberg and Tullis*, 1984; *Koch et al.*, 1989]. Hence the stresses derived from rheological data on basaltic rocks at least should be the correct order of magnitude.

Pore pressure in Earth is a poorly known quantity [*Carter and Tsenn*, 1987]. Figure 6 illustrates that power law creep equations predict exponentially rising stresses with declining temperature. Consequently, unless the pore fluid pressure is very high (greater than ~0.8 times lithostatic pressure), there will never be a direct transition from frictional sliding to power law creep in the simulations; the transitional rheology will be used instead.

Calculation of the stress and displacement proceeded column by column. The vertically integrated horizontal displacement in each column was specified by the horizontal velocity boundary condition and was partitioned throughout the column as determined by rheology, pressure, temperature, and stress. Because the hottest nodes in a given column are the weakest, most of the displacement occurs in the hottest nodes. This requires two imposed constraints. (1) In columns that contain an inverted thermal gradient, the displacement is constrained to occur above the base of the thermal inversion (i.e., in columns behind the leading edge of the subducted plate, the displacement was constrained to occur within the upper plate or within the basaltic layer of the lower plate). This is necessary to ensure that the horizontal velocity specified as a boundary condition occurs within the subduction zone, and not simply at the base of the peridotite layer. (2) In columns that lack an inverted thermal gradient (i.e., in columns ahead of the leading edge of the subducted plate), the displacement is constrained to occur within the upper 18 km. This 18-km constraint is necessary to ensure that the velocity specified as a boundary condition is not distributed over the thickness of the mantle, and is an artificial means for implicitly accounting for buoyancy of the subducted plate. It was also assumed that the stress required for power law creep was constant within any given column. This is a reasonable approximation because the thickness of the subduction zone (≤ 2 km) is much less than the column height (34 km). This stress was determined, by iteration, to be the stress that produced vertically integrated strain rates within the column that matched the imposed velocity boundary condition. All layers within the column that could deform by power law creep at such a stress were assumed to do so at the rate specified by their flow law; all other layers remained undeformed.

Calculation Procedures

A time step of 0.01 m.y. was used to ensure stability of the thermal calculations. Each time step was composed of the following:

1. Determine where any metamorphic reactions occur. Change rock types as appropriate, and add or subtract heat.
2. Allow heat to conduct.
3. Calculate the differential stress in each column that sustains the imposed horizontal velocity boundary condition.
4. Compute the resultant vertical gradient in the horizontal strain rate and displacement in each column.
5. Determine the amount of heat generated by deformational heating.

6. Move material to reflect the displacement gradient in each column.

7. Return to step 1.

The simulations were halted when the principal features of the metamorphic sole formed, and temperatures were low enough that the deformation was entirely brittle or transitional. The small time step means that the calculations are implicitly self-consistent (e.g., the correct interplay between deformational heating and stress is effectively maintained by iteration on a 0.01-m.y. time step).

RESULTS

Many simulations were conducted using the tectonic history suggested by *Lippard et al.* [1986]; two disparate models with young (5 m.y. old) and old (100 m.y. old) subducted lithosphere are shown here in detail. In both simulations, intraoceanic subduction was assumed to be initiated at the contact between young oceanic lithosphere and the lithosphere that it intruded. The young oceanic lithosphere was the Oman ophiolite and was 5 m.y. old at the time subduction begins. The older lithosphere was either 5 or 100 m.y. old at the time of subduction beneath the ophiolite, and consists of 100 km of oceanic lithosphere followed by 160 km of continental lithosphere. Both simulations were terminated when the temperatures in the fault zone are too low for power law creep and the principal features of the metamorphic sole have been produced. Moreover, a different mechanical model would be more appropriate to characterize the deformation, which had become dominantly brittle and transitional. Note that steady state has not been achieved, and models by *Peacock* [1987b] suggest that steady state will not be achieved for at least another 10 m.y.

Figures 7 and 8 illustrate series of time steps for subduction of 100-m.y.-old and 5-m.y.-old lithosphere beneath the ophiolite. The most obvious differences between Figures 7 and 8 are that the younger subducted material reaches higher temperatures, has a reduced degree of thermal inversion, and is metamorphosed more rapidly than the older material. None of these features is surprising but each has implications for deformation, which in turn affect metamorphism. Because the younger slab is hotter, a thicker zone of the fault deforms by power law creep. This also means that deformation occurs at lower stresses and slower strain rates for a given velocity, which minimizes the deformational heating compared to a colder slab. The fault zone also propagates downward more rapidly into a younger subducted slab, producing a thicker metamorphic sole. Dehydration occurs at an accelerated rate in younger, hotter lithosphere, removing heat from the subducted plate at an earlier stage. This causes the zone of brittle deformation to propagate downward more rapidly. Power law creep of the peridotite was generally restricted to temperatures greater than 750°C (power law creep at lower temperatures would require unreasonably high stresses; see Figure 6). Differential stresses in the peridotite just ahead of the subducted plate reached the imposed 200 MPa limit of the transitional deformation. Power law creep of the basaltic layer was limited to temperatures greater than 500°C. The differential stress supported by the basaltic layer in the fault zone was on the order of 100 MPa.

Figures 7c and 8d correspond to the time at which temperatures were low enough that the deformation was entirely brittle or transitional. At that time the base of the ophiolite contained an approximately 500-m-thick sole of greenschist-

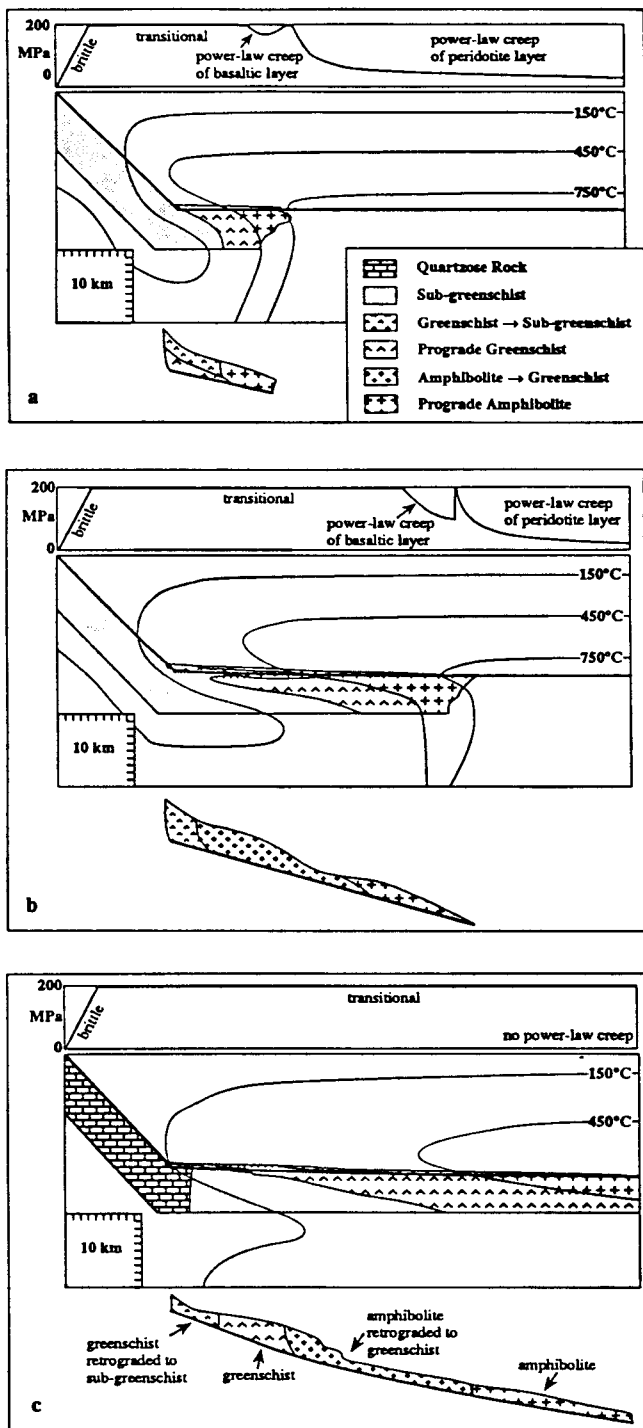


Fig. 7. A time sequence illustrating the temporal and spatial changes in temperature, rock types, and stress magnitudes calculated for subduction of 100-m.y.-old lithosphere beneath the ophiolite. The subduction velocity was initially 70 mm yr^{-1} and monotonically declines to 20 mm yr^{-1} within 5 m.y. The upper panels of each part of the figure show the differential stress supported by the rocks in the fault zone. The middle panels of each part of the figure show the temperature, rock type, and displacement fields. The different rock types in the basaltic layer of the subducted plate are shown with different patterns. The heaviest line indicates the depth at which the deformation is concentrated in each column (i.e., the fault zone). All material above and to the right of the fault zone is the ophiolite. Note that the fault zone begins in the bottom of the upper plate, and moves deeper into the lower plate with time, accreting a wedge of lower plate material to the upper plate. The lower panels of each part of the figure show the metamorphic sole with 10X vertical exaggeration for clarity. (a) 0.5 m.y. after subduction has begun. The total convergence is 34 km, and the convergence rate is 66 mm yr^{-1} . Ductile deformation in the peridotite layer ahead of the subducted slab occurs at differential stresses of $\sim 30 \text{ MPa}$. Where the peridotite is cooler ($< 750^\circ$), the deformation occurs at higher stresses. A narrow zone of power law creep occurs in the amphibolite-facies basaltic rocks near the leading edge of the subducted plate. (b) 1.0 m.y. after subduction has begun. The total convergence is 64 km, and the convergence rate is 62 mm yr^{-1} . (c) 2.0 m.y. after subduction has begun. The total convergence is 120 km, and the convergence rate is 50 mm yr^{-1} . The base of the ophiolite contains an approximately 500-m-thick sole of greenschist-facies rocks tapering eastward to a few hundred meters of amphibolite-facies rocks.

facies basaltic material (some of which was retrograded from amphibolite facies) and amphibolite-facies material, tapering to a few hundred meters of amphibolite-facies material.

During subduction, progressively deeper levels of the leading edge of the subducted plate come in contact with the upper plate, because the upper levels of the subducted plate accrete to the base of the ophiolite. In other words, first pelagic sedimentary rocks and upper lavas of the leading edge of the subducted plate accrete to the base of the ophiolite, later, lower lavas and dikes accrete, and so on, until accretion no longer occurs. In the simulations shown in Figures 7 and 8, $\sim 1500 \text{ m}$ of material have been removed from the leading edge of the subducted plate.

Temperature-time paths can be constructed for the upper and lower plates to illustrate their thermal evolution. Figure 9 shows the temperature-time paths for material initially at the leading edges of the upper and lower plates. In subducted lithosphere of 100 m.y. age, the thermal gradient remains essentially normal (i.e., the material at greater depths is hotter). Field investigations, however, show that the metamorphic rocks in the sole have an inverted metamorphic gradient. The resolution to this apparent paradox is that the lower plate has progressively accreted to the upper plate. Hence the lines in Figure 9 do not correspond to a single column of rock; the once-vertical column has been spread over a wide subhorizontal area. The temperature maxima in the -100 , -300 , -500 , and -700 curves correspond to the times at which material 100, 300, 500, and 700 m down in the lower plate accretes to the upper plate. The convergence of temperatures of material initially in the bottom of the upper plate and the top of the lower plate is evident in the shapes of curves labeled $+500$ and -100 . The lower layers of the subducted plate that did not accrete were simply subducted and heated to higher temperatures (curves -1200 and -1700). The originally lowest parts of the upper plate peridotite show continuous cooling (pale lines $+500$ and $+1500$).

The thermal histories of columns in a subducted plate of 5-m.y. age are different (Figure 9b). For example, layers -100 and -300 reach lower peak temperatures because the fault zone propagates down into the lower plate more quickly in the 5-m.y.-old plate than in the 100-m.y.-old plate, and the material accretes before it can reach high temperatures.

Figure 10 shows the P-T history of the leading edge of the subducted plate. The box shows the maximum P and T reached during amphibolite-facies metamorphism at the base of the Oman ophiolite, as estimated from thermobarometry [Ghent and Stout, 1981]. Neither simulation produces temperatures quite hot enough, but higher temperatures are sustained significantly longer in the 5-m.y.-old subducted plate.

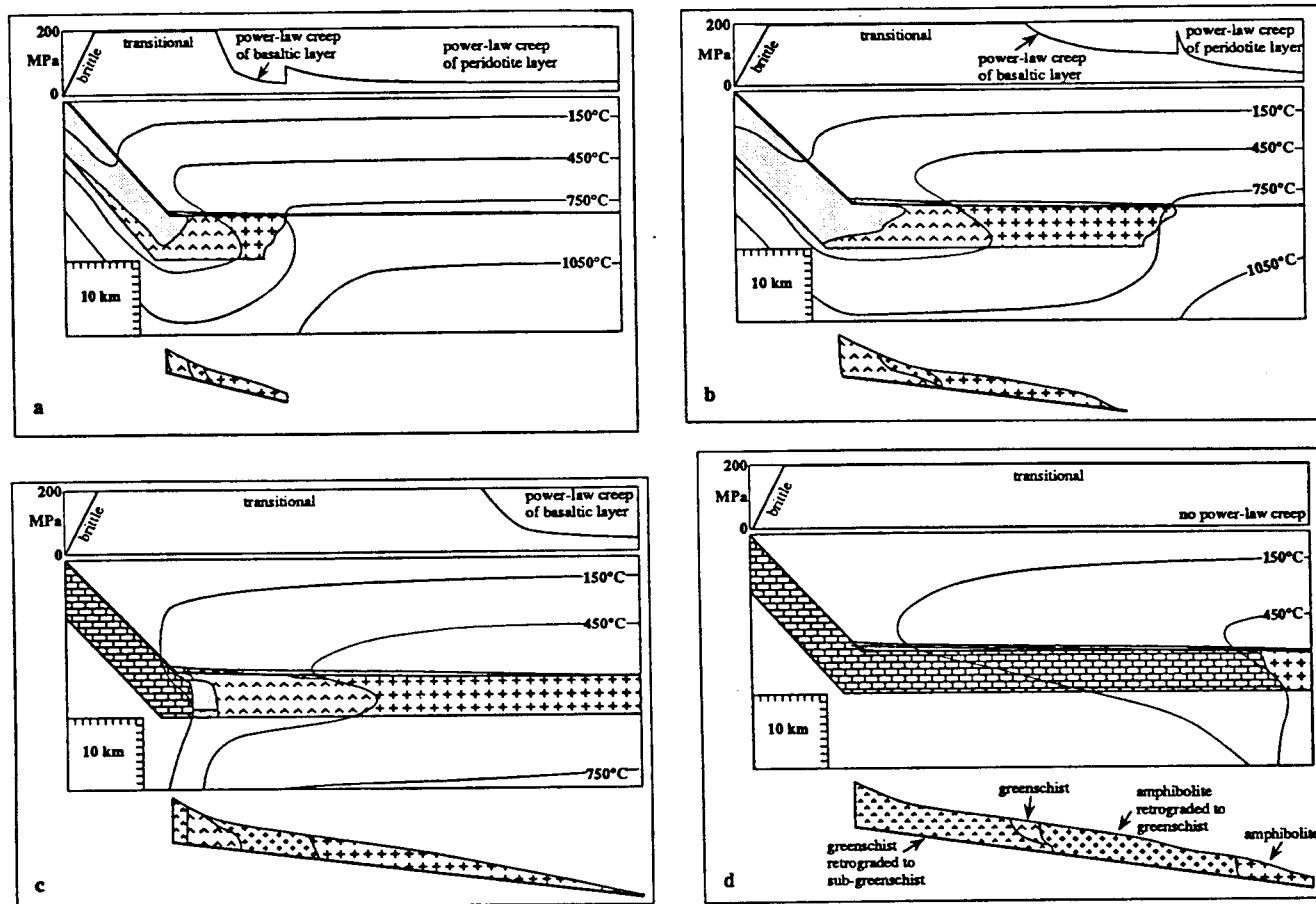


Fig. 8. A time sequence illustrating the temporal and spatial changes in temperature, rock types, and stress magnitudes calculated for subduction of 5-m.y.-old lithosphere beneath the ophiolite. Otherwise similar to Figure 7. (a) 0.5 m.y. after subduction has begun. The total convergence is 34 km, and the convergence rate is 66 mm yr^{-1} . (b) 1.0 m.y. after subduction has begun. The total convergence is 64 km, and the convergence rate is 62 mm yr^{-1} . (c) 2.0 m.y. after subduction has begun. The total convergence is 120 km, and the convergence rate is 50 mm yr^{-1} . (d) 3.5 m.y. after subduction has begun. The total convergence is 182 km, and the convergence rate is 35 mm yr^{-1} . The base of the ophiolite contains an approximately 500-m-thick sole of greenschist-facies rocks tapering eastward to a few hundred meters of amphibolite-facies rocks.

Sensitivity of the Model to Parameters

The influence of model parameters was evaluated by varying the value of each parameter while holding all other parameters constant. Specifically, a range of values for velocity, thermal conductivity, transitional deformation mechanism stress (maximum stress), and pore pressure were examined.

Increasing (decreasing) the subduction velocity reduces (increases) the length of time required to subduct a given amount of material. Consequently, heat advection gains importance relative to heat conduction. This means that for a given amount of subduction, the thermal gradient between the two plates is more extreme when subduction is rapid and less so when subduction is slow. For a slow subduction velocity, heat from the base of the upper plate is transferred more rapidly into the lower plate. Initially, this causes more rapid metamorphism of the lower plate basaltic material and more rapid downward progression of the fault zone. In the long term, however, thermal equilibration of the entire column causes the fault zone to cool to temperatures too low for dislocation creep. Deformational heating is reduced during slower subduction, which also tends to reduce the lifetime of the system.

Increasing (decreasing) the thermal conductivity increases

(reduces) the rate of heat conduction. When the thermal conductivity is increased, the subducted plate heats up more rapidly, and the upper plate cools more rapidly. Consequently, the subducted basaltic rocks undergo prograde metamorphism more rapidly and support smaller stresses when deforming. This produces interesting feedback among deformational heating, heating through metamorphic reactions, and thermal conduction. Smaller stresses produce less deformational heating, and more rapid prograde metamorphism means more rapid consumption of heat by dehydration reactions, but in the simulations this is nearly compensated by the increased thermal conduction.

Pore pressure ratios less than 0.9 all produce roughly similar results because the frictional sliding stress exceeds the transitional stress (200 MPa differential stress) at shallow depths where temperatures are too cool for power law creep. At pore pressures ≥ 0.9 , the frictional sliding stress never exceeds the transitional stress, and there is a direct change from frictional sliding to power law creep. Such pore pressures were considered to be unreasonably high for young basaltic and ultramafic rocks.

In simple terms, increasing (decreasing) the transitional stress reduces (increases) the number of nodes that deform by

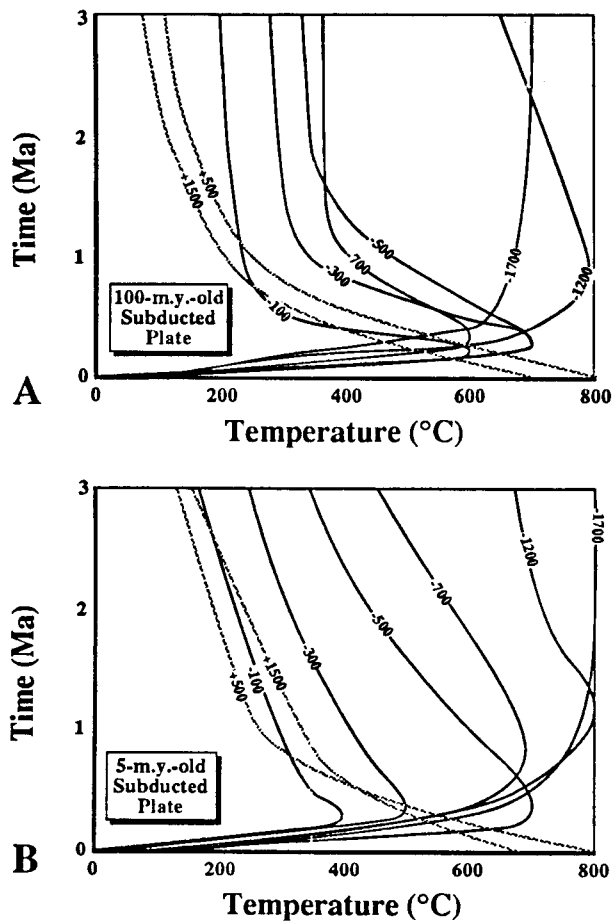


Fig. 9. Temperature histories for the leading column of the subducted plate (heavy lines) and the leading column of the over-riding plate (light lines). The labels -100 through -1700 indicate the temperature histories of rocks initially in the lower plate 100-1700 m below the initial depth of the fault zone. The labels +500 and +1500 indicate rocks initially in the upper plate 500 and 1500 m above the initial depth of the fault zone. At -0.5 m.y., rocks initially in the lower plate follow a spectrum of T-t paths between two divergent end-member paths. Lower parts of the basaltic layer (paths -1200 and -1700) continue to be subducted and are continually heated. Higher parts of the basaltic layer (paths -100, -300, -500, and -700) accrete to the base of the upper plate and cool off.

frictional sliding or crystal plasticity. More importantly, a higher ceiling on the stress increases deformational heating, and this retards the rate at which the upper plate cools and speeds the rate at which the lower plate is metamorphosed.

DISCUSSION

The following section discusses why metamorphic rocks accrete to the base of Tethyan-type ophiolites. This explanation considers the instantaneous placement and thrusting of a column of one plate against another, which is different from the dynamic two-dimensional model presented earlier, but it illustrates the interaction between deformation and metamorphism in the sole in a highly simplified fashion. Figure 11 shows a fault zone between two moving plates, the upper plate ophiolite and the lower subducted plate. Consider a one-dimensional column through both plates (Figure 11a). The initial thermal gradient is a sawtooth, and deformation occurs at the base of the peridotite where the peridotite deforms by power law creep at stresses lower than those required for brittle

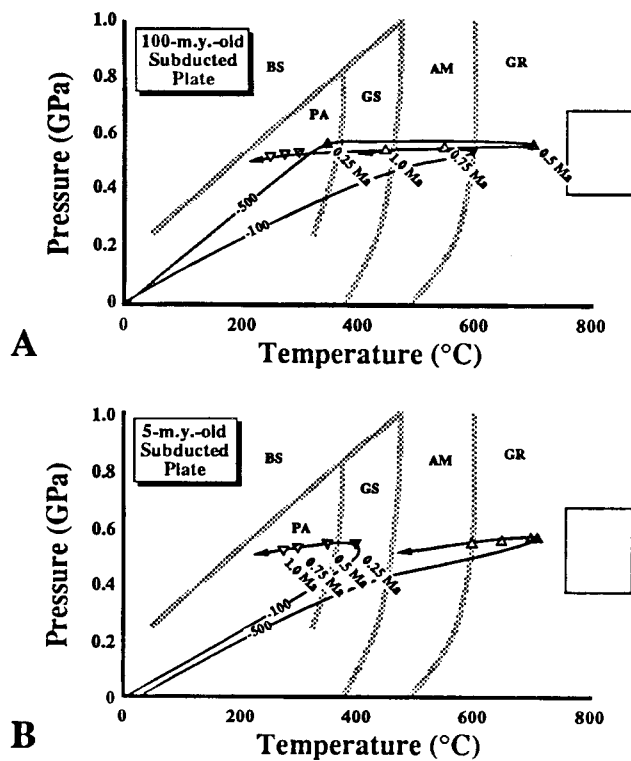


Fig. 10. Pressure-temperature histories of the metamorphic sole. The curve labels are like those in Figure 9. Temperatures and pressures at 0.25-m.y. intervals are shown by differently shaded symbols. BS, blueschist facies; PA, pumpellyite-actinolite and prehnite-pumpellyite facies; GS, greenschist facies; AM, amphibolite facies; GR, granulite facies. The rectangle illustrates peak pressures and temperatures estimated by *Ghent and Stout* [1981] for the amphibolite-facies basaltic rocks in Oman. (a) Subducted plate is 100 m.y. old (corresponds to Figures 7 and 9a). (b) Subducted plate is 5 m.y. old (corresponds to Figures 8 and 9b). The decompression histories shown are purely arbitrary and were included only to separate the cooling histories of these layers for easier viewing.

behavior. As thermal conduction occurs, the thermal gradient relaxes, and the upper portion of the lower plate basaltic layer is metamorphosed to greenschist facies (Figure 11b). The stress supported during power law creep of greenschist is greater than the stress for frictional sliding, so deformation continues only in the upper plate peridotite, although cooling of the upper plate causes the deformation to be concentrated in a narrower band. At a later time, the lower plate reaches amphibolite-facies conditions, and is then warm enough for power law creep to occur at stresses lower than those for brittle behavior (Figure 11c). In these three steps, the zone of deformation moved progressively downward into the warming lower plate, and upper parts of the lower plate basaltic layer successively accreted to the base of the ophiolite.

IMPLICATIONS

The results of the simulations presented here suggest the following. All aspects of the simulations agree with field relationships in Oman, except for point 7 below. Moreover, several predictions can be made that can be tested by further field work in Oman. It must be emphasized that these conclusions result from simulations based on many assumptions.

1. The sole of the Oman ophiolite should contain an

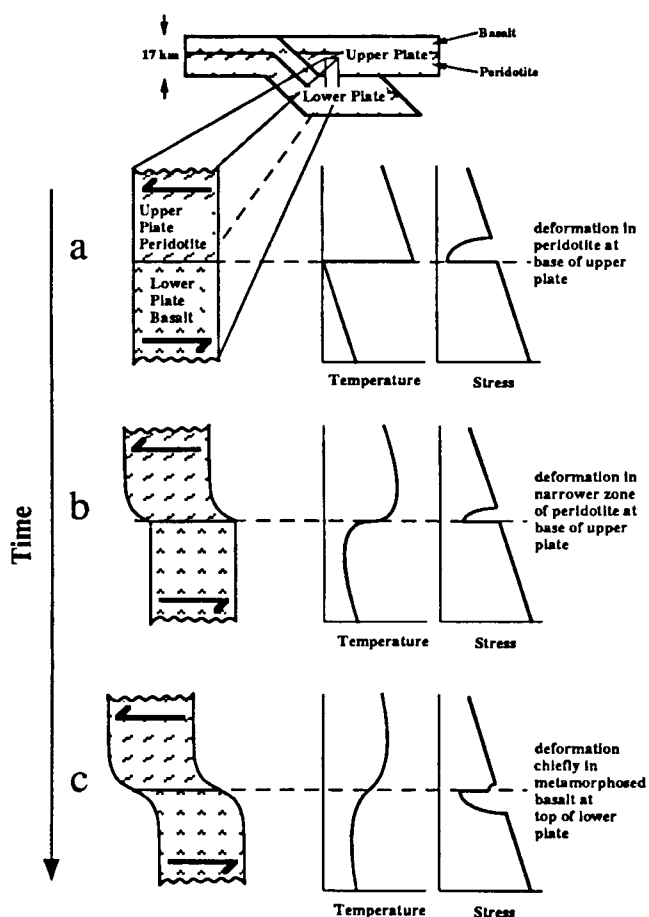


Fig. 11. One-dimensional cartoon of how conductive decay of a sawtooth-shaped thermal gradient can produce localized deformation at progressively deeper levels, resulting in accretion of metamorphic rocks to the base of the ophiolite. Steps in Figures 11a, 11b, and 11c represent a time sequence.

inverted metamorphic gradient from amphibolite facies to greenschist facies (Figure 8).

The Oman ophiolite does contain an inverted metamorphic field gradient from anatectic material to greenschist facies. Material in the simulations did reach temperatures high enough for melting, but melting was not specifically modeled. This inverted metamorphic field gradient exists because the higher grade rocks were not completely retrogressed to lower grade assemblages.

2. The amphibolite-facies and greenschist-facies rocks in Oman should attain a maximum thickness of ~500 m, with thicker exposures toward the leading edge of the ophiolite tapering toward thinner exposures near the trailing edge. Amphibolite-facies rocks should be more prevalent toward the trailing edge of the ophiolite, and greenschist-facies rocks should be more prevalent toward the leading edge (Figure 9).

The thickness of the metamorphic sole produced in the simulations is similar to that observed in Oman, several hundred meters each of greenschist- and amphibolite-facies. The metamorphic field gradient parallel to the emplacement direction (i.e., the lateral change from amphibolite to greenschist facies) produced in the simulations has not been reported from the Oman ophiolite. If future investigations in Oman show the existence of a horizontal metamorphic field gradient that is parallel to the emplacement direction, then this

study provides a physical explanation of how the gradient develops. Further, the emplacement direction of other Tethyan-type ophiolites may be inferable from the horizontal component of the metamorphic field gradient.

It is important to note that this horizontal metamorphic field gradient can exist only if higher grade rocks are not completely retrogressed to lower grade assemblages. If retrogression does occur, however, there should still be a horizontal gradient in the cooling ages recorded by minerals such as amphibole and mica.

3. Metamorphic rocks in the sole of the Oman ophiolite should have formed along pressure-temperature paths like those in Figure 10.

Jamieson [1986] produced pressure-temperature paths for the metamorphic sole of the St. Anthony Complex, a Tethyan-type ophiolite in Newfoundland, using mineral chemistries and parageneses to estimate the pressures and temperatures. The temperature paths produced in this study are qualitatively similar. Studies of P-T paths of metamorphic rocks from Oman, using Gibbs' method and inclusion thermobarometry [e.g., Spear and Selverstone, 1983], could test the temperature history predictions of this study and estimate the pressure history.

Tethyan-type ophiolites are an extreme example that metamorphic field gradients need not preserve the thermobarometric gradient that was present during the metamorphism [e.g., Spear and Selverstone, 1983]. This is true for regional metamorphic terranes because minerals in different portions of the metamorphic field gradient may have formed at different times. In Tethyan-type ophiolites, however, deformation plays an important role. The metamorphic field gradients in the metamorphic soles of Tethyan-type ophiolites are a sequence of rocks that developed at different pressures and temperatures in disparate areas at different times and were amalgamated into a single column during subduction.

4. Peak temperatures during amphibolite-facies metamorphism of the Oman ophiolite sole should have been ~700°C. Some amphibolite-facies rocks should have been overprinted by greenschist-facies parageneses (Figure 9).

The temperatures (765°-875°C) estimated by Ghent and Stout [1981] from the metamorphic sole in Oman are not significantly above the peak metamorphic temperature achieved in the simulations. Some amphibolite-facies rocks in Oman were overprinted by greenschist-facies parageneses.

5. The lower few hundred meters of the peridotite above the metamorphic sole in Oman should contain a foliation formed at temperatures of ~800°C (Figure 9).

The lower 150-2000 m of the peridotite in Oman contain a mylonitic foliation that increases in intensity downward [Searle et al., 1980; Nicolas et al., 1980; Boudier and Coleman, 1981; Boudier et al., 1988; Ceuleneer et al., 1988]. Boudier and Coleman [1981], Lippard et al. [1986], and Ceuleneer et al. [1988] inferred that the temperatures of mylonitization were 750°-1000°C. The simulations in this study suggest that the downward increase in the intensity of the foliation can be attributed to the progressive downward movement of the fault zone and narrowing of the fault zone (see Figure 7). The simulations suggest that this foliation formed at differential stresses >30 MPa. Although stress magnitudes at some stages of the emplacement of the Oman ophiolite could possibly be estimated through microstructural paleopiezometry, such measurements have not yet been reported for any ophiolite.

6. The amphibolite-facies and greenschist-facies rocks

grown during the early stages of emplacement of the Oman ophiolite should be foliated. The foliation in the amphibolite should have formed by crystal-plastic deformation of the constituent minerals.

The metamorphic rocks in Oman are gneisses and schists formed during crystal-plastic deformation of constituent minerals. The latest greenschist-facies minerals grew during static conditions, presumably after movement along the sole thrust ceased.

7. The amphibolite-facies rocks in the Oman ophiolite sole should have been metamorphosed during a ~1-3 m.y. interval; the greenschist-facies rocks required more than 3 m.y. for formation.

This is perhaps the greatest disagreement between the predictions of the simulations and the field geology. Most K-Ar and $^{40}\text{Ar}/^{39}\text{Ar}$ ages indicate that much of the amphibolite-facies metamorphism in Oman spanned ~6 m.y., and the greenschist-facies metamorphism ~14 m.y. [Alleman and Peters, 1972; Searle et al., 1980; Lanphere, 1981; Montigny et al., 1988]. Perhaps the ophiolite was even younger than 5 m.y., as suggested by Boudier and Nicolas [1988], or perhaps the metamorphism occurred in different areas of the ophiolite at different times, implying a more complicated emplacement history.

8. Rocks in the metamorphic sole near the leading edge of the Oman ophiolite should be metamorphosed pelagic sedimentary rocks and upper pillow lavas, while rocks near the trailing edge of the ophiolite should be lower lavas and sheeted dikes.

No horizontal spatial variation in the protoliths of the metamorphic sole rocks has been reported from the Oman ophiolite. If future investigations in Oman show the existence of horizontal spatial variations in rock types, then this study provides a physical explanation of how the variation developed. Further, such spatial variation in rock type might also be used in other Tethyan-type ophiolites to infer the emplacement direction. If this is true, then such spatial variation in rock type might also be used in other Tethyan-type ophiolites to infer the emplacement direction.

Future studies might produce more realistic models of ophiolite emplacement by addressing some of the simplifications in the present model.

CONCLUSIONS

The production and accretion of metamorphic rocks at the base of Tethyan ophiolites can be explained in terms of a physical model incorporating laboratory measurements of rheological and thermal properties. The temperature, stress, rock type, and displacement fields during ophiolite emplacement were modeled to understand the interaction between deformation and metamorphism. The metamorphic rocks are produced because cool basaltic rocks are subducted beneath warmer peridotite; they accrete to the base of the ophiolite because the sole thrust propagates downward from the peridotite into the basaltic rocks in response to the downward conduction of heat. The differential stress supported by basaltic material in the fault zone was on the order of 100 MPa (50 MPa maximum shear stress). The lithosphere subducted beneath the Oman ophiolite was probably young (~5 m.y. old) rather than older (~100 m.y. old), as suggested by the peak metamorphic temperatures preserved in the amphibolite-facies rocks of the sole thrust. The metamorphic field gradients in the soles of Tethyan-type ophiolites are a sequence of rocks developed at

different pressures and temperatures in disparate areas at different times that were amalgamated into a single column. The metamorphic field gradient along the sole thrust may have hotter peak temperatures near the leading edge of the ophiolite and cooler peak temperatures near the trailing edge. The soles may also show systematic spatial variation in rock types, from pelagic sedimentary rocks and upper lavas near the leading edge of the ophiolite, to lower lavas and dikes toward the trailing edge of the ophiolite. These criteria might successfully be applied to determine the emplacement direction of other Tethyan-type ophiolites.

Acknowledgments. The finite difference algorithm was borrowed from Peter Bird. The manuscript benefitted from reviews by Gray E. Bebout, Francoise Boudier, Richard T. Chen, David S. Diamond, Harry W. Green II, David V. Kemp, James C. Sample, An Yin, and an anonymous JGR reviewer.

REFERENCES

- Alabaster, T., J. A. Pearce, and J. Malpas, The volcanic stratigraphy of the Oman ophiolite complex, *Contrib. Mineral. Petrol.*, **81**, 168-183, 1982.
- Alleman, F., and T. Peters, The ophiolite-radiolarite belt of the North Oman Mountains, *Ecol. Geol. Helv.*, **65**, 657-697, 1972.
- Anderson, R. N., S. Uyeda, and A. Miyashiro, Geophysical and geochemical constraints at converging plate boundaries, Part I, Dehydration in the downgoing slab, *Geophys. J. R. Astron. Soc.*, **44**, 333-357, 1976.
- Béchenec, F., J. Le Metour, D. Rabu, M. Villey, and M. Beurrier, The Hawasina basin: A fragment of a starved passive continental margin, thrust over the Arabian platform during obduction of the Semail nappe, *Tectonophysics*, **151**, 323-343, 1988.
- Bird, P., Finite element modeling of lithosphere deformation: The Zagros collision orogeny, *Tectonophysics*, **50**, 307-336, 1978.
- Borch, R.S., and H.W. Green II, Deformation of peridotite at high pressure in a new molten salt cell: Comparison of traditional and homologous temperature treatments, *Phys. Earth Planet. Inter.*, **55**, 269-276, 1989.
- Boudier, F., and R. G. Coleman, Cross section through the peridotite in the Semail ophiolite, southeastern Oman Mountains, *J. Geophys. Res.*, **86**, 2573-2592, 1981.
- Boudier, F., and A. Nicolas (Ed.), The ophiolites of Oman, special issue, *Tectonophysics*, **151**, 1-401, 1988.
- Boudier, F., G. Ceuleneer, and A. Nicolas, Shear zones, thrusts and related magmatism in the Oman ophiolite: Initiation of thrusting on an oceanic ridge, *Tectonophysics*, **151**, 275-296, 1988.
- Brace, W. F., and D. L. Kohlstedt, Limits on lithospheric stress imposed by laboratory experiments, *J. Geophys. Res.*, **85**, 6248-6252, 1980.
- Byerlee, J. D., Brittle-ductile transition in rocks, *J. Geophys. Res.*, **73**, 4741-4750, 1968.
- Caristan, Y., The transition from high temperature creep to fracture in Maryland diabase, *J. Geophys. Res.*, **87**, 6781-6790, 1982.
- Carmichael, R. S. (Ed.), *CRC Handbook of Physical Properties of Rocks*, vol. III, 340 pp., CRC Press, Boca Raton Fl., 1984.
- Carter, N.L., and M.C. Tsenn, Flow properties of continental lithosphere, *Tectonophysics*, **136**, 27-63, 1987.
- Ceuleneer, G., A. Nicolas, and F. Boudier, Mantle flow patterns at an oceanic spreading center: The Oman peridotites record, *Tectonophysics*, **151**, 1-26, 1988.
- Christensen, N.I., and J.D. Smewing, Geology and seismic structure of the northern section of the Oman ophiolite, *J. Geophys. Res.*, **86**, 2545-2555, 1981.
- Clark, S. P., Handbook of Physical Constants, *Mem. Geol. Soc. Am.*, **97**, 587 pp., 1966.
- Coleman, R. G., and C. A. Hopson (Ed.), The Oman ophiolite special section, *J. Geophys. Res.*, **86**, 2495-2782, 1981.
- Durham, W. B., V. V. Mirkovich, and H. C. Heard, Thermal diffusivity of igneous rocks at elevated pressure and temperature, *J. Geophys. Res.*, **92**, 11615-11634, 1987.
- Emewin, M., C. Pflumio, and H. Whitechurch, The death of an accretion zone as evidenced by the magmatic history of the Semail ophiolite (Oman), *Tectonophysics*, **151**, 247-274, 1988.

- Ghent, E. D., and M. Z. Stout, Metamorphism at the base of the Samail ophiolite, southeastern Oman Mountains, *J. Geophys. Res.*, **86**, 2557-2571, 1981.
- Glennie, K. W., M. G. A. Boeuf, M. W. Hughes-Clark, M. Moody-Stuart, W. F. H. Pilar, and B. M. Reinhardt, Geology of the Oman Mountains, *Verh. K. Ned. Geol. Mijnbouwkd. Genoot. Ged. Ser.*, **31**, 423, 1974.
- Goffé, B., A. Michard, J. R. Kienast, and O. Le Mer, A case of obduction-related high-pressure, low-temperature metamorphism in upper crustal nappes, Arabian continental margin, Oman: P-T paths and kinematic interpretation, *Tectonophysics*, **151**, 363-386, 1988.
- Hacker, B. R., and J.M. Christie, Brittle/ductile and plastic/cataclastic transitions in experimentally deformed and metamorphosed amphibolite, in *The Brittle-Ductile Transition, The Heard Volume, Geophys. Monogr. Ser.*, AGU, Washington, D.C., in press, 1990.
- Hacker, B.R., A. Yin, J.M. Christie, and A.W. Snoke, Differential stress, strain rate, and temperatures of mylonitization in the Ruby Mountains, Nevada: Implications for the rate and duration of uplift, *J. Geophys. Res.*, in press, 1990.
- Hadizadeh, J., and E.H. Rutter, The low temperature brittle-ductile transition in quartzite and the occurrence of cataclastic flow in nature, *Geol. Rundsch.*, **7**, 493-509, 1983.
- Hansen, F. D., Semibrutle creep of selected crustal rocks at 1000 MPa, Ph.D. dissertation, 224 pp., Tex. A&M Univ., College Station, 1982.
- Hansen, F. D. and N. L. Carter, Creep of selected crustal rocks at 1000 MPa, *Eos Trans. AGU*, **63**, 437, 1982.
- Helgeson, H. C., J. M. Delany, H. W. Nesbitt, and D. K. Bird, Summary and critique of the thermodynamic properties of rock-forming minerals, *Am. J. Sci.*, **278A**, 229 pp., 1978.
- Jamieson, R. A., P-T paths from high temperature shear zones beneath ophiolites, *J. Metamorph. Geol.*, **4**, 3-22, 1986.
- Jaoul, O., J. A. Tullis, and A. K. Kronenberg, The effect of varying water contents on the creep behavior of Heavtree quartzite, *J. Geophys. Res.*, **89**, 4298-4312, 1984.
- Kirby, S. H., Rheology of the lithosphere, *Rev. Geophys.*, **21**, 1458-1487, 1983.
- Koch, P.S., J.M. Christie, A. Ord, and R.P. George Jr., Effect of water on the rheology of experimentally deformed quartzite, *J. Geophys. Res.*, **94**, 13,975-13,996, 1989.
- Kronenberg, A. K., and J. A. Tullis, Flow strengths of quartz aggregates: Grain size and pressure effects due to hydrolytic weakening, *J. Geophys. Res.*, **89**, 4281-4297, 1984.
- Lanphere, M. A., K-Ar ages of metamorphic rocks at the base of the Samail ophiolite, Oman, *J. Geophys. Res.*, **86**, 2777-2782, 1981.
- Lippard, S. J., A. W. Shelton, and I. G. Gass, The ophiolites of northern Oman, *Mem. Geol. Soc. London*, **11**, p. 178, 1986.
- Manghni, M.H., and R.G. Coleman, Gravity profiles across the Samail ophiolite, *J. Geophys. Res.*, **86**, 2509-2525, 1981.
- Montigny, R., O. Le Mer, R. Thuizat, and H. Whitechurch, K-Ar and $^{40}\text{Ar}/^{39}\text{Ar}$ study of the metamorphic rocks associated with the Oman ophiolite, *Tectonophysics*, **151**, 345-362, 1988.
- Moores, E. M., Origin and emplacement of ophiolites, *Rev. Geophys.*, **20**, 735-760, 1982.
- Newmark, R.L., R.N. Anderson, D. Moos, and M.D. Zoback, Structure, porosity and stress regime of the upper oceanic crust: Sonic and ultrasonic logging of DSDP hole 504B, *Tectonophysics*, **118**, 1-42, 1985.
- Nicolas, A., F. Boudier, and J. L. Bouchez, Interpretation of peridotite structures from ophiolitic and oceanic environments, *Am. J. Sci.*, **280A**, 192-210, 1980.
- Nicolas, A., G. Ceuleneer, F. Boudier, and M. Misseri, Structural mapping in the Oman ophiolites: Mantle diapirism along an oceanic ridge, *Tectonophysics*, **151**, 27-55, 1988.
- Ord, A., and J.M. Christie, Flow stresses from microstructures in mylonitic quartzites of the Moine Thrust zone, Assynt area, Scotland, *J. Struct. Geol.*, **6**, 639-654, 1984.
- Pallister, J. S., and C. A. Hopson, Samail ophiolite plutonic suite: Field relations, phase variation, cryptic variation and layering, and a model of a spreading ridge magma chamber, *J. Geophys. Res.*, **86**, 2593-2645, 1981.
- Parsons, B. P., and J. G. Sclater, An analysis of the variation of ocean floor bathymetry and heat flow with age, *J. Geophys. Res.*, **82**, 803-827, 1971.
- Peacock, S. M., Creation and preservation of subduction-related inverted metamorphic gradients, *J. Geophys. Res.*, **92**, 12,763-12,781, 1987a.
- Peacock, S. M., Thermal effects of metamorphic fluids in subduction zones, *Geology*, **15**, 1057-1060, 1987b.
- Pearce, J. A., T. Alabaster, A. W. Shelton, and M. P. Searle, The Oman ophiolite as a Cretaceous arc-basin complex: evidence and implications, *Philos. Trans. R. Soc. London, Ser. A*, **300**, 299-317, 1981.
- Penrose Conference Participants, Penrose field conference on ophiolites, *Geotimes*, **17**, 24-25, 1972.
- Poirier, J. -P., *Creep of Crystals*, 260 pp., Cambridge University Press, New York, 1985.
- Robertson, A. H. F., and N. H. Woodcock, Genesis of the Batinah mélange above the Samail ophiolite, Oman, *J. Struct. Geol.*, **5**, 1-17, 1983a.
- Robertson, A. H. F., and N. H. Woodcock, Zabyat Formation, Samail Nappe, Oman: Sedimentation on to an emplacing ophiolite, *Sedimentology*, **30**, 105-116, 1983b.
- Searle, M. P., S. J. Lippard, J. D. Smewing, and D. C. Rex, Volcanic rocks beneath the Samail ophiolite nappe in the northern Oman Mountains and their significance in the Mesozoic evolution of the Tethys, *J. Geol. Soc. London*, **137**, 589-604, 1980.
- Shelton, G. L., and J. Tullis, Experimental flow laws for crustal rocks, *Eos Trans. AGU*, **62**, 396, 1981.
- Sibson, R.H., Roughness at the base of the seismogenic zone: contributing factors, *J. Geophys. Res.*, **89**, 5791-5799, 1984.
- Spear, F. S., and J. Selverstone, Quantitative P-T paths from zoned minerals: Theory and tectonic applications, *Contrib. Mineral. Petrol.*, **83**, 348-357, 1983.
- Thomas, V., J. P. Pozzi, and A. Nicolas, Paleomagnetic results from Oman ophiolites related to their emplacement, *Tectonophysics*, **151**, 297-321, 1988.
- Tilton, G. R., C. A. Hopson, and J. E. Wright, Uranium-lead isotopic ages of the Samail ophiolite, Oman, with applications to Tethyan ocean ridge tectonics, *J. Geophys. Res.*, **86**, 2763-2775, 1981.
- Toksöz, M. N., J. W. Minear, and B. R. Julian, Temperature field and geophysical effects of a downgoing slab, *J. Geophys. Res.*, **76**, 1113-1138, 1971.
- Toksöz, M. N., S. C. Solomon, J. W. Minear, and D. H. Johnston, Thermal evolution of the moon, *The Moon*, **4**, 190-213, 1972.
- Tullis, J., and R. A. Yund, Transition from cataclastic flow to dislocation creep of feldspar: Mechanisms and microstructures, *Geology*, **15**, 606-609, 1987.
- Williams, H., and W. R. Smyth, Metamorphic aureoles beneath ophiolite suites and alpine peridotites: tectonic implications with West Newfoundland examples, *Am. J. Sci.*, **273**, 594-621, 1973.
- Woodcock, N. H., and A. H. F. Robertson, The upper Batinah Complex, Oman: Allochthonous sediment sheets above the Samail ophiolite, *Can. J. Earth Sci.*, **19**, 1635-1656, 1982a.
- Woodcock, N. H. and A. H. F. Robertson, Stratigraphy of the Mesozoic rocks above the Samail ophiolite, *Geol. Mag.*, **119**, 67-76, 1982b.

B.R. Hacker, Department of Geology, Stanford University, Stanford CA 94305.

(Received June 12, 1989;
revised November 3, 1989;
accepted November 9, 1989.)